Astron. Astrophys. 323, 183–188 (1997)

ASTRONOMY
AND
ASTROPHYSICS

Subtle structures in the wind of P Cygni

F. Vakili, D. Mourard, D. Bonneau, F. Morand, and Ph. Stee

Observatoire de la Côte d'Azur, Département Fresnel, CNRS URA 1361, GI2T, F-06460 Saint Vallier de Thiey, France

Received 16 October 1996 / Accepted 18 December 1996

Abstract. The blue super-giant P Cygni has been observed with the Grand Interféromètre à 2 Télescopes (GI2T). Using high spatial resolution data at low spectral resolution *(R=3860)* of Hα and HeI6678 emission lines we clearly resolve the extended enveloppe of this Luminous Blue Variable on August 1994. The angular diameter of the equivalent uniform disk taken over the total extent of these lines corresponds to $\Phi_{H\alpha}$ = 5.52 $\pm$ 0.47 and Φ_{He} = 2.48 $\pm$ 2.16 mas respectively. We also analysed spectrally-resolved fringes in both lines for 3.4 Å width narrow channels across the emission profiles. Based on robust calibrations from two reference stars γ Lyr and α Cep we detect subtle spatial structures throughout P Cyg's wind. First: we find that the maximum extension of P Cyg occurs at -130 km.s^{-1}. This value agrees well with a picture of P Cyg where matter is radially blown outward according to the classical theory of P Cyg line profiles. Secondly: we detect a significant local phase-shift of the fringe signal at -208 km.s^{-1} which corresponds to an angular separation of 0.8 mas from the continuum source. This is interpreted as a localized blob of moving gas with enhanced brightness whose position is about 4 photospheric radii to the south of P Cyg's underlying star.

Key words: stars: interstellar matter – stars: individual P Cyg – lines: profiles – stars: mass loss – techniques: interferometric

1. Introduction

P Cyg (B1Iape, V=4.9) is an intriguing massive star which exhibits spectacular emission lines and temporal variations (Lamers 1986). As the prototype of Luminous Blue Variables (Conti 1984) it has received considerable attention both from the theoreticians and observers (Davidson 1986, de Groot&Lamers 1992, Stahl et al. 1995). Despite a globally coherent picture derived from extensive spectroscopic and photometric studies, little has been done until now on P Cyg with high angular resolution techniques such as adaptive optics or long baseline interferometry (de Vos 1992, Nishimoto et al. 1994). Recently it has been claimed that a single interferometric observation could tightly constrain the physics of P Cyg's wind (Burgin&Chalabaev 1992, hereafter BC), provided it were observed simultaneously at high spectral resolution. This is exactly what is being reported hereafter on the basis of long baseline interferometry of P Cyg in Hα and HeI6678 emission lines. In the followings we briefly describe the observational material and data analysis focusing our attention on calibration procedures. Then we show the new constraints that our measurements bring on the morphology of P Cyg that we interpret as subtle structures in the kinematics of its wind.

Send offprint requests to: Farrokh Vakili

2. Instrumentation and observations

The present work was carried on the GI2T stellar interferometer described in two recent papers (Mourard et al. 1994a, Mourard et al. 1994b). Following earlier attempts (Mourard et al. 1992) we obtained a single interferometric baseline on August 4th 1994 on P Cyg and the reference star γ Lyr (B9III, V=3.2). On both stars, the dispersed fringes were recorded in two simultaneous spectral channels centred on Hα and HeI6678. The effective resolving power of the GI2T spectrograph was calibrated on a neon laboratory source as 1.7Å at the mean λ=6560Å. The radial velocities were determined using a heliocentric correction of -16 km.s^{-1} (Scuderi et al. 1996). All interferometric recordings were obtained while the fringes were tracked by the real-time RAFT system and it is worth to remind that to date, P Cyg is the faintest object observed with a long baseline optical interferometer at the level of 1 angstrom spectral resolution (Koechlin et al. 1996).

3. Data analysis and calibration

We reduced our data following the cross-spectral density method applied to previous studies of Be stars on the GI2T (Stee et al. 1995). In a preliminary step, we computed long exposures ($\approx$30min) from 20 ms spectro-interferograms recorded by the photon-counting camera CP40. The projection of this long exposure on the dispersion axis provides a low dispersion spectrum of the star including Hα and HeI6678. After flat-fielding, we determined the total extent of lines for carrying two different studies. In a first approach we cross-correlate a wide continuum band with 1) the line taken over its total width, 2) a continuum band taken over the same width as the line. In a second approach (hereafter referred as IDI for Interferometric Doppler-Imaging), we compute the cross-correlation of a wide

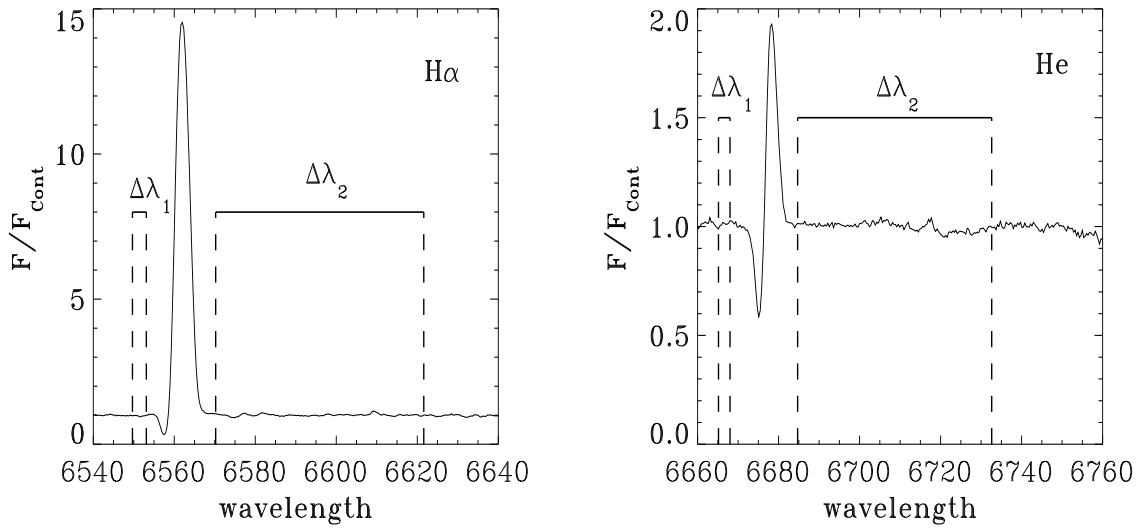

Fig. 1. Low resolution spectra of P Cyg of Hα and HeI6678 emission lines recorded by the GI2T on August 4th 1994. $\Delta\lambda_1$ and $\Delta\lambda_2$ correspond to the bandwidths used for cross-correlating the interferometric signal between line and continuum channels.

Table 1. Journal of observations of P Cyg and reference stars γ Lyr and α Cep in 1994. The last 3 columns give the average Universal Time of the observation, the baseline projected on the sky in meters and the spatial frequency in cycle.arcs^{-1} for the wavelength of 6560 Å.

Star	HD	Date	UT	Baseline	Sp. Freq.
γ Lyr	176437	94/8/4	21:38	50.1	370.1
P Cyg	193237	94/8/4	22:57	17.7	130.8
α Cep	203280	94/8/6	23:50	27.5	203.2

continuum channel with a series of narrow channels across the emission line. This is repeated by spectral shifts of 1.7 Å for both channels from the blue to the red wing of the line starting and finishing in the continuum. The narrow and wide spectral channels are $\Delta\lambda_1$=3.4 Å and $\Delta\lambda_2$=50 Å respectively (Fig. 1). Since the signal to noise ratio in the cross-correlations depends on the geometric mean of the number of photons in $\Delta\lambda_1$ and $\Delta\lambda_2$, the interferometric signal can be safely estimated in the narrow channel even if the flux or the fringe visibility are very small in this channel. This applies in particular to the absorption component of Hα in P Cyg where the number of photons is dramatically small.

By Fourier transforming the cross-correlations we obtain the cross-spectral density (CS) between the 2 channels from which we can estimate both the visibility and phase of the objective cross-spectrum. This can be understood as follows:

$$< CS_{12} >=< \widetilde{I}_{\lambda_1} \widetilde{I}^*_{\lambda_2} > \quad (1)$$

where $<>$ refers to the ensemble average, $\widetilde{I}_{\lambda_i}$ refers to the Fourier transform of short exposures in the spectral channel $\Delta\lambda_i$, * to the complex conjugate. CS_{12} is a complex quantity and can be developped into:

$$< CS_{12} >= |\widetilde{O}_1||\widetilde{O}_2|e^{i\Delta\psi}T_{12} \quad (2)$$

where $|\widetilde{O}_i|$ denotes the normalized spatial power spectrum of the source in $\Delta\lambda_i$, $\Delta\psi$ the objective phase-gradient and T_{12} the cross-spectral OTF. Now T_{12} depends on λ_2-λ_1 and can strongly vary with atmospheric conditions (Berio et al. 1996). However, normalizing the continuum-line CS on the continuum-continuum CS yields a turbulence-independant estimate of the objective power spectrum in λ_1 and λ_2. The argument of T_{12} includes the average optical path difference (OPD) during the total duration of the recording. Obviously, the average OPD differs from star to star depending on the general observing conditions of the GI2T and the atmosphere. Plotting the argument of CS versus the Doppler-shift along the dispersion axis informs -to the first order- on the projected North-South astrometric position of the object relative to the continuum star. The measure of this differential phase is theoretically limited by photon-noise (Petrov, 1988), so that super-resolution effects down to μarcsecond level could be attained with decametric baselines. Clearly, our first approach provides an estimate of the angular diameter of P Cyg envelope taken over the total width of the emission line, whilst the second IDI approach enables us to sound its envelope kinematics.

4. Results

4.1. Angular diameter of P Cyg in Hα and HeI6678

We assume P Cyg as a point-source in the continuum on the basis of a detailed study of its basic parameters (Lamers et al. 1983) which estimates the photospheric angular diameter as 0.4 ± 0.1 mas at a distance of d = 1.8 $\pm$ 0.1 kpc for R_*=76 $\pm$ 15$R\odot$. According to our first approach, we find the normalized visibilities as $V_{H\alpha}$ = 0.48 $\pm$ 0.07 and V_{He} = 0.88 $\pm$ 0.20. These values correspond to equivalent uniform disk diameters of $\Phi_{H\alpha}$ = 5.52 ± 0.47 and Φ_{He} = 2.48 ± 2.16 mas respectively. For a uniform disk, the error quoted on the diameter is directly obtained by deriving $V(\Phi) \propto J_1(\Phi)/\Phi$, i.e. $\delta\Phi/\Phi \propto \delta V(\Phi)/J_2(\Phi)$, where $J_2(\Phi)$ is the Bessel function of the first kind and second order.

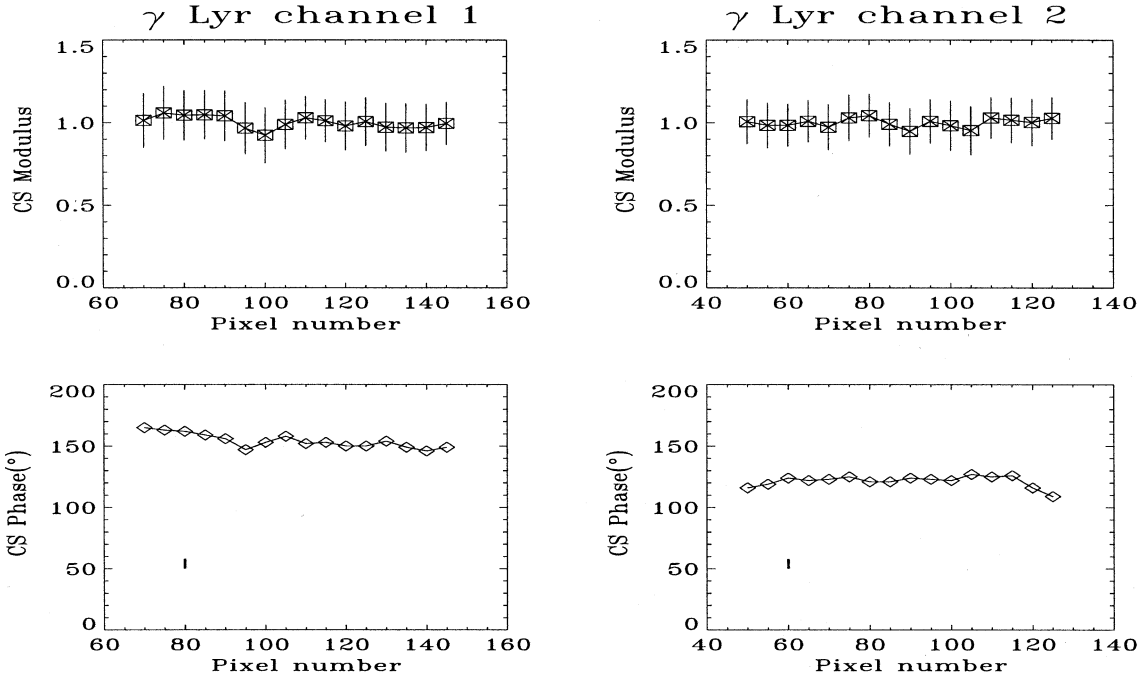

Fig. 2. Results of Interferometric-Doppler-Imaging on γ Lyr. Left panel: CP40 channel 1 (reference for Hα), right panel: CP40 channel 2 (reference for HeI6678). Modulus (top) and phase (bottom) of the cross-spectrum between the continuum and line channels as a function of pixel number parallel to the dispersion axis. The errors, corresponding to 1σ, on the moduli and on the phase-gradient (typically 8°, left corner of phase plots at the size of diamond symbols) are estimated from the actual photon-statistics in the cross-spectral density of short exposures and other artifacts due to the detector response.

4.2. Super-resolution effect in the wind of P Cyg

As described in Sect. 3, slicing the profile in narrow spectral channels informs on the dimension and spatial position of P Cyg as a function of Doppler-shift across the line. More explicitly, this position corresponds to the difference of angular position between the photocentre of iso-radial-velocity areas of P Cyg with that Doppler-shift and the position of the continuum source. We first applied our method to the reference star γ Lyr in the continuum region of 6000 ± 200 Å, in order to determine the effect of the detector response on the measure of the fringe phase-gradient. It can be seen from Fig. 2 that the modulus and phase of CS for γ Lyr remain constant (within the error bars) as a function of the pixel number on both channels of CP40. These channels were later used to recording Hα and HeI6678 fringes on P Cyg the same night as γ Lyr and the comparison star α Cep on august 6th. Fig. 3 and 4 depict the results of our IDI analysis applied to these two stars.

For α Cep, relative visibilities and phases remain constant within the error bars on both Hα and HeI6678. This means that α Cep's size and position are identical in the continuum and in Hα which is not surprising on regard of its spectral type and angular diameter of 1.48 ± 0.07 mas (Malagnani and Morossi, 1990). In comparison, the modulus of P Cyg visibility undergoes a continuous and asymmetrical variation across Hα where a minimum visibility occurs at -130 km.s^{-1}. The phase gradient is marked by a negative bump of 37°at -208 km.s^{-1} with respect to its average value of 130°. 37°at the 17.7 m baseline at λ=6560 Å correspond to an angular shift of 0.8 mas on the sky towards the south direction. This absolute orientation is determined from the relative phase of the interference signal in the dispersed fringes of the GI2T. In other words the projected position of those regions of P Cyg envelope having a radial velocity of -208 ± 78 km.s^{-1} is displaced by 0.8 mas from the continuum source of the star. This could witness for a decentred envelope around the photosphere of P Cyg or for a bright blob of gas whose north-south projected position is separated by about 4 stellar radii from the central source of P Cyg. In comparison, the variation of relative visibility and phase of P Cyg across HeI6678 remain marginal as a function of Doppler-shift meaning that the fine structures of the HeI emitting envelope are essentially unresolved at the 17.7 m baseline. This is not so surprising since the higher photo-ionization potential of HeI makes emission occur closer to the central star than for HI.

In order to establish the robustness of our phase-bump interpretation in Hα we carried the IDI analysis on γ Lyr for two other nights centered on this line. We found that the behaviour of the phase-gradient versus Doppler-shift for γ Lyr is similar to that of α Cep depicted in Fig. 3 (left-bottom plot). A refined analysis of the phase showed that the instabilities of the detector response as a function of pixel are likely to produce additional errors on phase-gradient determinations. Therefore the errors quoted on CS phase as estimated from photon-noise alone are under-estimated and approach more realisticly 8°which is the standard deviation of the phase-gradient on reference stars as a function of Dollper-shift. Hence, our phase-bump detection on

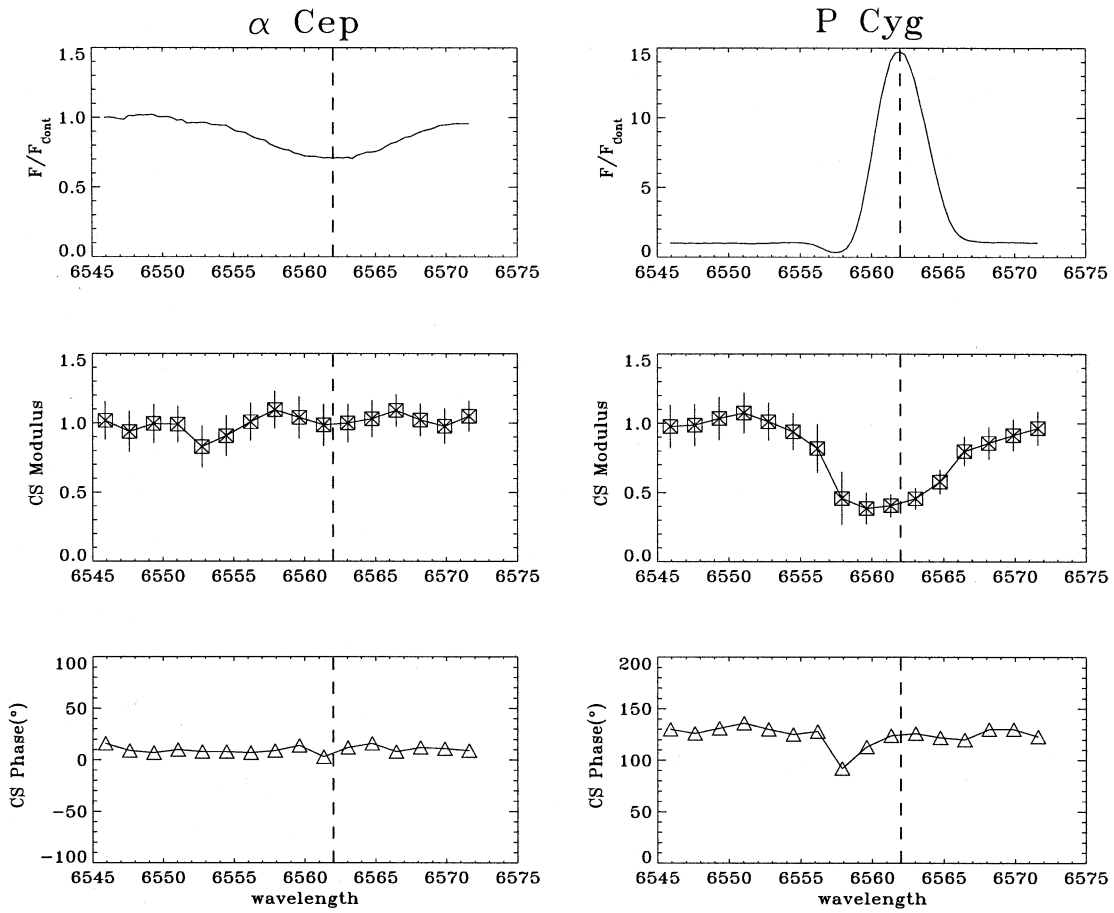

Fig. 3. Results of IDI analysis of P Cyg (right panel) and the reference star αCep (left panel). Top: profiles of the Hα line. Middle and bottom: modulus and phase of the cross-spectrum between the continuum and line channels as a function of Doppler-shift across Hα. The error bars on CS moduli and phase follow the same definition as for Fig. 2.

P Cyg at -208 ± 78 km.s^{-1} (centered on maximum absorption) is determined better than 4σ.

5. Discussion

In their model for P Cyg using the Sobolev approximation, Burgin&Chalabaev (1992) computed spectral Hα profiles and the effective radius R_{eff} of the envelope as a function of Doppler-shift. They examined two models based on an isothermal envelope at T=12750K and secondly on an outward temperature-drop from 18000K to 10000K. Both models use density and velocity laws depending on $(1 - R_*/R)^\gamma$ where γ=4 (Drew 1985). BC obtained the variation of envelope radius versus Doppler-shift. They predicted that the maximum extent of the envelope occurs around -230 km.s^{-1} whereas we find -130 km.s^{-1}. These values do not significantly disagree on regard of our IDI spectral channel width of 3.4 Å. Amazingly enough, the asymmetrical shape of BC's curve giving the envelope size across the Hα profile agrees with the relative visibility estimate from our data (compare their Fig. 2 to the present Fig. 3). Qualitatively speaking, this does not condradict the fact that P Cyg at blue-shifted wavelengths must look like a ring with a dark center due to the stellar-wind absorption. In their exact numerical solution of the radiative transfer based on Sobolev approximation, BC define R_{eff} as the equivalent radius of the star+envelope system in Hα. Such a definition slightly over-estimates the angular extent of the blue-shifted P Cyg compared to its true intensity distribution across the sky.

Note that BC's predicted Hα extent of P Cyg can be inferred from its average monochromatic angular diameter across the line, i.e. 10 and 15 photospheric radii for the isothermal and non-isothermal models respectively. Our estimate of $\Phi_{H\alpha} = 5.52 \pm 0.47$ corresponding to $R_{H\alpha}/R_* = 13.8 \pm 4.6$ cannot disentangle between BC's two models. During our run the Hα peak intensity attained 15 times the local continuum Fig. 3). The same peak predicted by BC's models attains 10 times the continuum for the temperature-drop model, slightly better than the isothermal scenario which is $\sim$8.5. We emphasize that our estimates of P Cyg envelope in Hα and HeI6678 as $\Phi_{H\alpha} = 5.52 \pm 0.47$ and $\Phi_{He} = 2.48 \pm 2.16$ mas do not overlap at 1σ and could tightly constrain the velocity-density structure of P Cyg wind, although that would need a quantitative modelling of P Cyg beyond the scope of this paper. To be more effective, this demands a more accurate estimate of the HeI envelope size only achievable by longer interferometric baselines of the GI2T.

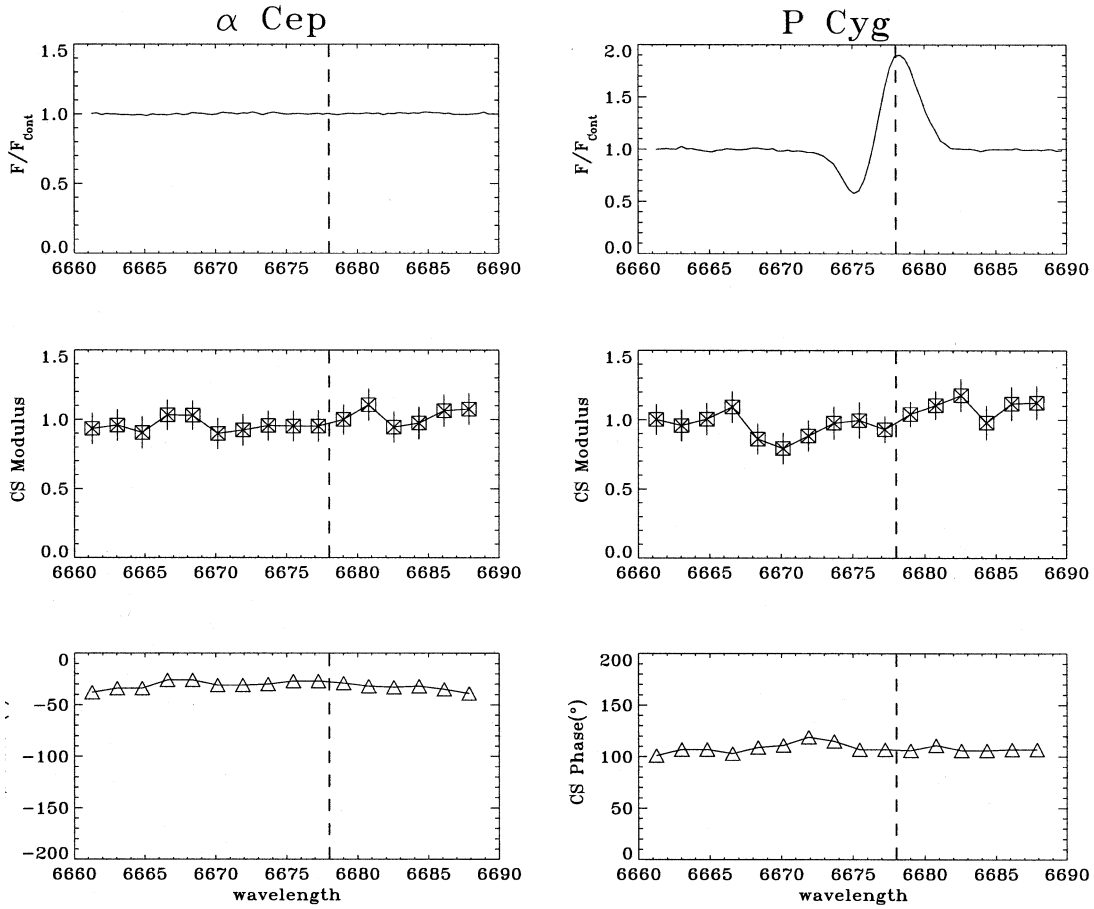

Fig. 4. Results of IDI analysis on P Cyg (right panel) and the reference star αCep (left panel). Top: profile of the HeI6678 line. Middle and bottom: modulus and phase of the cross-spectrum between the continuum and line channels as a function of Doppler-shift across the line. The error bars on CS moduli and phase follow the same definition as for Fig. 2.

Also note that, due its large uncertainty, the estimated HeI6678 radius (Fig. 5) is rather indicative: for instance $\Phi_{He} - 1\sigma \approx \Phi_*$.

The BC model is the first numerical code simulating the observable parameters of P Cyg as they are measured by a spectro-interferometer such as the GI2T. None of the numerous models for P Cyg -BC's included, account for anisotropies in the wind of this super-giant (Najarro, 1995 and references therein). The subtle phase effect found by us across the Hα profile strongly suggests that anisotropic structures actually occur at the basis of the wind of P Cyg. We think that this phase effect is more likely produced by a localized spatial feature in the wind of P Cyg at $4R_*$ from its photosphere, rather than a decentred envelope mentionned in Sect. 4.2. In the latter case the phase effect would have been apparent across the whole Hα profile, whereas we measure a single bump at -208 km.s^{-1}. The $4R_*$ value must be taken somehow as a minimum, since the measured phase-gradient gives the projected separation on the North-South direction due to GI2T's baseline. The uncertainty on the separation can further be constrained by adopting velocity laws through the wind of the form $v(r) = v_0 + (v_\infty - v_0)(1 - R_*/R)^\gamma$. Taking 15 and 300 km.s^{-1} for photospheric and terminal velocities and γ=4 (Drew 1985), the wind would attain 105 km.s^{-1} at $4R_*$. For smaller values of γ, say γ=1, $v(4R_*)$=198 km.s^{-1} which is comparable to the -208 km.s^{-1} local bump that we detect. Since the spatial brightness distribution of P Cyg, as seen by the observer, depends only on the impact parameter (see BC's model for instance) one would not expect to see an asymmetrical phase effect for a steep acceleration of the wind due to γ=1. Therefore P Cyg's outflow must follow a much smoother velocity law depending on γ=3 to 4. Similarly, the localized feature cannot be at a large distance since it would be at the local speed of the outflow and would not produce the phase-gradient bump. We conclude that the true separation of the local feature is rather small placing it close to the photosphere (on regard of the overall dimension of the envelope), probably at the boundary of the HeI sphere. Finally we believe that the detection of such feature must be related to some energetic mechanism speculated as a jet originating at the photosphere and producing a localized anisotropy in the density-velocity field at the basis of P Cyg wind.

The existence of strong inhomogeneities at the surface of the central LBV stars are foreseen by the theory of non-radial pulsation, shock waves or other instability mechanisms such as turbulent photospheric motions (de Jager 1984). Localized

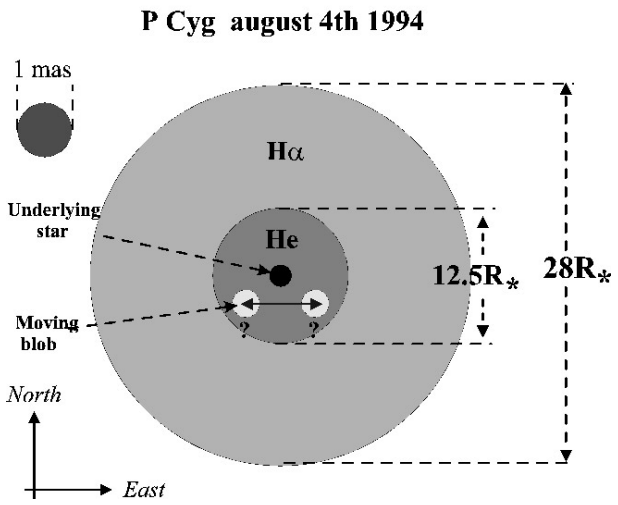

Fig. 5. Schematic morphology of P Cyg wind projected on the sky according to GI2T's observations. The extent of Hα and HeI6678 envelopes are given in units of photospheric radius assumed as $76 \pm 15 R\odot$ and corresponding to 0.4 mas. The angular scale is given as 1 mas (top-left) taking a distance of 1.8 ± 0.1 kpc. The projected position of the detected blob is at 4 stellar radii to the south of P Cyg central star but its absolute position in the east-west direction remains unknown.

density enhancement in the wind of massive stars should result in measurable polarimetric or spectroscopic variability at the level of 1% (Richardson et al. 1996, Barlow et al. 1994) but becomes more easily detectable when spatial information is added to spectral information (and vice-versa). As recently modeled for Be stars (Stee, 1996), the measure of interferometric phase effect, can disentangle between different velocity laws in the wind of hot stars which would be otherwise undetectable by spectroscopy or from the amplitude of the fringe signal alone. On the other hand large spatial structures resolved as blobs out to a few arcseconds have been reported around P Cyg in Hα and NII nebular lines (Johnson et al. 1992). In principle, one could check if the large-scale blobs were in some way the *echo* of inner inhomogeneities by coordinated monitoring of P Cyg by long baseline interferometry and adaptive optics on 2-4m class telescopes. The follow-up of propagating wind instabilities by multi-resolution imaging would be most effective if it were carried using spectral resolution as well. In this context, the subtle structure at mas spatial resolution reported by the present work is the premice of a new approach to the understanding of P Cyg wind and LBV stars in general, against which theories of the dynamical evolution of the circumstellar gas around massive stars could be checked (Garcia-Seguria et al. 1996).

Acknowledgements. We are grateful to Emeric Le Floch for assisting the observations, to A. Blazit, L. Koechlin and I. Tallon-Bosc for the operation of the CP40, the RAFT fringe-tracker and the optical beam-combiner of the GI2T. Earlier discussions with M. de Groot and A. Chalabaev have much stimulated P Cyg observations. We are grateful to J. Pachéco, J.M. Le Contel and A. Labeyrie for having reviewed the original manuscript. We also acknowledge O. Stahl for his constructive refereeing of the paper. This work was supported by PNHRAA-INSU and the CNRS organization GDR-Milieux Circumstellaires.

References

Barlow, M.J., Drew, J.E., Meaburn, J., Massey, R.M., 1994, MNRAS, 268, L29-L34
Berio, P., Mourard, D., Vakili, F., et al., 1997, JOSA-A, vol. 14, No. 1
Burgin M.S. and Chalabaev A.A., 1992, ESA Colloquium n targets for Space-based Interferometry, ESA SP-354, 185-187
Conti, P.S., 1984, in *Observational Tests of Stellar Evolution Theory*, IAU Symposium 105, eds. A. Maeder and A. Renzini (Dordrecht, Reidel), p.233
Davidson K., 1986, in *Instabilities in Luminous Early Type Stars*, eds. Lamers and de Loore, D. Reidel Publishing Company, pp127-142
Garcia-Segura, G., Lac Low, M-M., Langer, N., 1996, A&A, 305, 229-244
de Groot, M.J.H, Lamers, H.J.G.L.M., January 1992, Nature, 355, 422-423
de Jager C., 1984, A&A, 138, 246
de Vos M., 1992, *Optical Interferometry with SCASIS*, PhD. Dissertation. University of Groningen, The Netherlands
Drew J.E., 1985, MNRAS, 217, 867
Johnson, Dean R.H., Barlow, M.J., Drew, J.E., et al., 1992, MNRAS, 255, 261
Koechlin, L., Lawson, P., Mourard, D, et al., 1996, Applied Optics, 35, 16, 3002-3009
Lamers H.J.G.L.M., 1986, in *Instabilities in Luminous Early Type Stars*, eds. Lamers and de Loore, D. Reidel Publishing Company, pp99-126
Lamers, H.J.G.L.M., de Groot, M., Cassatella, A., 1983, A&A, 128, 299-310.
Malagnani, M.L., Morossi, C., 1990, A&AS, 85, 1015
Mourard, D., Blazit, A., Bonneau, D., et al., 1992, in *High-Resolution Imaging by Interferometry*, ESO Conference, March 1988, Garching, ed. F. Merkle., pp707-714, Garching, Germany
Mourard, D., Tallon-Bosc, I., Blazit, A., et al., 1994a, A&A, 283, 705
Mourard D., Tallon-Bosc I., Rigal F. et al., 1994b, A&A, 288, 675
Najarro F., 1995, PhD Thesis, *Quantitative Optical and Infrared Spectroscopy of Extreme Luminous Blue Supergiants*, Ludwig-Maximilian University, Munich. Germany.
Nishimoto, D., Africano, J., Morossi, C., et al., 1994, Bulletin of AAS, 185, dec., 1455-1456
Ochsenbein, F., and Halbwachs, J.L., 1982, A&AS, 47, 523
Petrov R., 1988, in *High-Resolution Imaging by Interferometry*, ESO Conference, March 1988, Garching, ed. F. Merkle., pp235-248, Garching, Germany
Richardson, L.L., Brown, J.C., Simmons, J.F.L., 1996, A&A, 306, 519
Scuderi, S., Bonnano, G., Spadaro, D. et al., 1994, ApJ, 437, 465-475
Stahl, O., Mandel, H., Wolf, B. et al., 1993, A&ASS, 99, 167
Stee, P., De Araujo, F.X., Vakili, F. et al., 1995, A&A, 300, 219
Stee P., 1996, A&A, 311, 945

This article was processed by the author using Springer-Verlag LaTeX A&A style file *L-AA* version 3.